Low-loss Ti:$LiNbO_3$ intersecting waveguides

Niraj Agrawal[a] and L. McCaughan
Department of Electrical and Computer Engineering, University of Wisconsin, Madison, Wisconsin 53706

(Received 11 November 1988; accepted for publication 7 February 1989)

Interactions between guided and radiation modes are studied experimentally in Ti:$LiNbO_3$ single-mode, single-Δn intersecting waveguides with small angles. These measurements, which cannot be interpreted in terms of any previous theory for intersecting waveguides, can be understood in terms of a recently developed multiple scattering analysis. Furthermore, it is found that the radiation losses in optical switches and crossovers can be dramatically reduced by a fractional doping of the intersection region.

Intersecting waveguides provide considerable flexibility in the design of guided-wave optical devices. Small and large intersection angles offer the possibility of making switches and crossovers, respectively.[1,2] However, until recently the mechanism of radiation losses in this geometry was not understood. In the following we present the radiation loss measurements on single-Δn (i.e., a uniform index everywhere in the guiding region) intersecting waveguides with small ($\theta < 2°$) angles. [Loss measurements in the same geometry for large ($\theta > 2°$) intersection angles have been reported previously.[2]] The experimental data are compared with the multiple scattering analysis[3,4] to elucidate the physical processes which give rise to radiation losses. The new insights attained due to the agreement between theory and experiment suggest that the radiation losses in optical switches and crossovers can be dramatically reduced by a fractional doping of the intersection region.

Single-mode waveguides were fabricated in z-cut $LiNbO_3$ with intersection angles in the range 0.3°–2.0° (see Fig. 1). The desired pattern of titanium strips with 6 μm width and 670 Å nominal thickness for single-Δn intersecting waveguides was defined using lift-off lithography. The titanium diffusion was carried out for 6 h at 1050 °C under flowing oxygen and water vapor. Light from an InGaAsP laser diode at 1.28 μm was endfire coupled into and out of waveguides in the TM mode using microscope objectives. The guided output light was imaged (magnified near-field pattern of fundamental mode with full width at half maximum of ~0.5 mm) onto a 1-mm-diam pinhole germanium photodetector. It follows from Fig. 1 that the power in the bar ($\eta_=$) and the cross ($\eta_\times$) states relative to a straight waveguide are given by P_B/P_E and $\sqrt{P_C/P_E}$, respectively. Therefore, the fraction of power lost per junction due to radiation is

$$\eta_{\text{rad}} = 1 - \eta_= - \eta_\times. \tag{1}$$

The radiation losses measured in this manner for small ($0.3° < \theta < 2.0°$) intersection angles are shown in Fig. 2. Note that as the intersection angle varies from 0.3° to 2.0°, the radiation loss first increases, reaches a local maximum, and then decreases. A second peak similar to the one reported here is predicted and observed in the regime of large intersection angles.[5] Thus, the phenomenon of radiation loss in intersecting waveguides exhibits a doubly peaked characteristic. These measurements cannot be interpreted in terms of any previous theory. For example, in case of single-Δn intersecting waveguides, the mode interference analysis[1,6] ignores the radiation losses and the beam propagation analysis[7] predicts a monotonic decrease in loss with an increase in intersection angle.

The nature of radiation loss in intersecting waveguides as described above can be understood in terms of multiple scattering analysis. In order to simplify this analysis, the slab (TE) geometry is used to model the titanium-diffused channel (TM) waveguides in lithium niobate. Note that the TE (TM) modes of a slab waveguide are physically equivalent to the TM (TE) modes of a channel waveguide. The total electric field E is decomposed into fields E_1 and E_2 associated with the individual waveguides (see inset of Fig. 1). Since a guided wave is launched from the left of the junction (at infinity) in waveguide 1, the zeroth-order scattered fields are given as

$$E_1^{(0)} = \Psi_1, \tag{2a}$$

$$E_2^{(0)} = 0, \tag{2b}$$

where $\psi_{1,2}$ represent the eigenfunctions of waveguides 1 and 2 corresponding to TE_0 mode. In the presence of a coupling between the two waveguides, the nth order scattered fields $E_i^{(n)}$ with $i = 1, 2$ generated in sequence ..., $E_2^{(n)}$, $E_1^{(n)}$,... for $n \geqslant 1$ are expressed as [4]

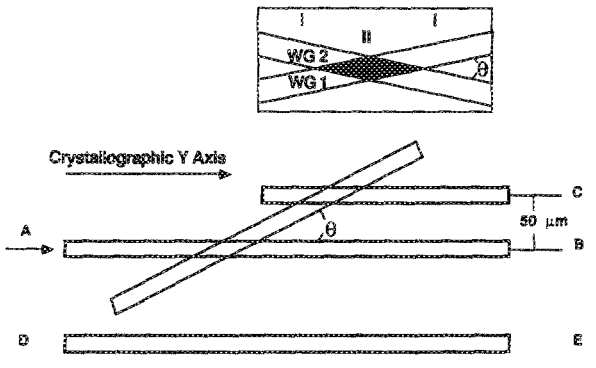

FIG. 1. Schematic diagram of the experimental geometry for Ti:$LiNbO_3$ intersecting waveguides along with a straight waveguide reference. Inset: regions I and II of intersecting waveguides where the latter is shown shaded to indicate its fractional doping.

[a] Present address: IBM Research Division, Almaden Research Center, 650 Harry Road, San Jose, CA 95120-6099.

 0003-6951/89/171669-03$01.00

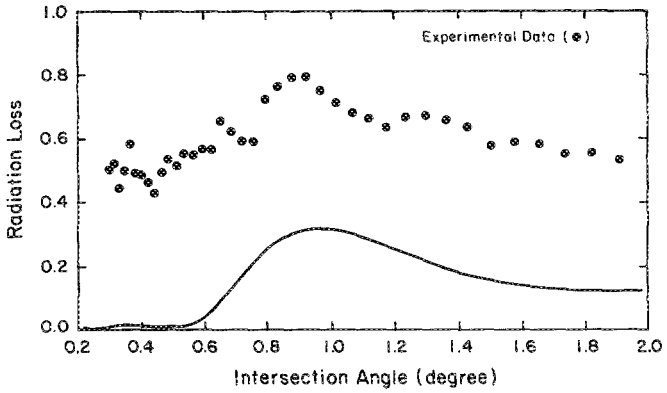

FIG. 2. Measured (referenced to straight waveguide) and calculated (normalized to incident power) radiation loss as a function of intersection angle for single-Δn intersecting waveguides.

$$E_2^{(n)} = [(W_2W_1)^n \quad {}^1W_2]\Psi_1, \tag{3a}$$

$$E_1^{(n)} = [(W_1W_2)^n]\Psi_1. \tag{3b}$$

The scattering operator W_i associated with the individual waveguides ($i = 1, 2$) is decomposed into two suboperators as

$$W_i = U_i + V_i, \tag{4}$$

where U_i and V_i generate guided and radiation fields of ith waveguide from the operand fields. The electric field (E_i) in either waveguide is obtained as a sum of fields ($...,E_i^{(n)},...$) due to the infinite sequence of scattering interactions as

$$E_i = \sum_{n=0}^{\infty} E_i^{(n)}. \tag{5}$$

A complete analysis taking all these interactions into account is not possible, so we resort to simplifying approximations. The first order ($n = 1$) scattered electric field in waveguide 2 is given by Eqs. (3) and (4) as

$$E_2^{(1)} = [U_2 + V_2]\Psi_1. \tag{6}$$

The interactions represented by Eq. (6) are $g(1) \rightarrow g(2)$ and $g(1) \rightarrow r(2)$, where $g(i)$ and $r(i)$ are used to denote guided and radiation fields of the ith waveguide. The calculated radiation losses as a function of intersection angle based on this interaction are compared to measurements in Fig. 2. The waveguide parameters, namely, half-width $a = 2\ \mu$m, substrate index $n_s = 2.300$, and film index $n_f = 2.305$, are selected for numerical analysis throughout this letter so as to represent well-confined single-mode waveguides in lithium niobate at a wavelength $\lambda = 1.3\ \mu$m. Note that the calculated radiation losses are shifted to lower values with respect to the experimental data. As discussed later, this approximately constant shift is due to having neglected the higher order guided-guided and guided-radiation mode scattering interactions. Aside from such discrepancy, a semiquantitative agreement between experiment and theory is obtained.

Recall that a first-order scattering theory was compared to the experiment for intersecting waveguides with small angles (Fig. 2). In this regime of operation the interaction between guided modes [$g(1) \leftrightarrow g(2)$] corresponds to several coupling lengths. Therefore, the incident power is scattered into the guided and radiation modes of both waveguides. In order to incorporate this physics we must consider higher order scattering interactions given by Eqs. (3) and (4). Although the evaluation of all such interactions is tedious if not impractical, it is instructive to examine the outcome of an improved analysis. Note that in Eqs. (3a) and (3b) the composite scattering operators W_iW_j with $i = 2, j = 1$ and $i = 1$, $j = 2$ act repeatedly. The action of these operators on an arbitrary operand field f is expressed using Eq. (4) as

$$W_iW_jf = [U_iU_j + V_iU_j + U_iV_j + V_iV_j]f, \tag{7}$$

where the second-order scattering interactions given by Eq. (7) are $f \rightarrow g(j) \rightarrow g(i)$, $f \rightarrow g(j) \rightarrow r(i)$, $f \rightarrow r(j) \rightarrow g(i)$, and $f \rightarrow r(j) \rightarrow r(i)$. In the last two terms, the radiation fields act as sources for subsequent scattering. The evaluation of these terms requires knowledge of the radiation fields everywhere in space. Since no expression is available for radiation fields except in the asymptotic limit, it becomes difficult to proceed beyond the first-order analysis. If, however, the effect of radiation fields as sources is ignored in subsequent scattering interactions, the nth order scattered fields can be evaluated for all n. In this approximation the fields associated with waveguides 2 and 1 are given by using Eq. (5) as

$$E_2 = i\sin(K)\Psi_2 + V_2[\cos(K)\Psi_1], \tag{8a}$$

$$E_1 = \cos(K)\Psi_1 + V_1[i\sin(K)\Psi_2], \tag{8b}$$

where K is the integrated coupling coefficient between the guided modes of two waveguides.[3]

The power coupled to the guided mode of waveguide 2 calculated in this manner for single-Δn intersecting waveguides is shown in Fig. 3 along with the corresponding experimental data. Note that the number of quasiperiods or peaks is in good agreement with the experiments, although the calculated amplitude of oscillations in the coupled power is overestimated. This last fact is not surprising because the ignored source terms (U_iV_jf) modify the amplitude of guided modes to account for the radiation loss. Moreover, the mode-interference analysis predicts only half as many quasiperiods as in Fig. 3, a fact which constitutes a firm evidence of its inadequacy even at small angles.[8] The subsequent analysis (computationally intensive) for radiation loss under the same approximation [see Eq. (8)] does not lead to any closer agreement with the measurements than what is shown in

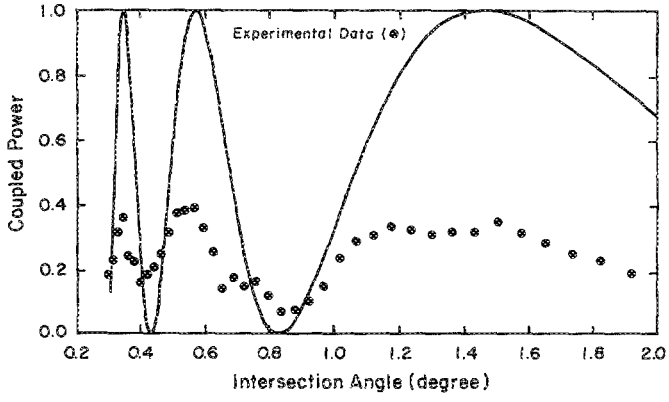

FIG. 3. Measured and calculated coupled power from waveguide 1 to 2 as a function of intersection angle for single-Δn intersecting waveguides.

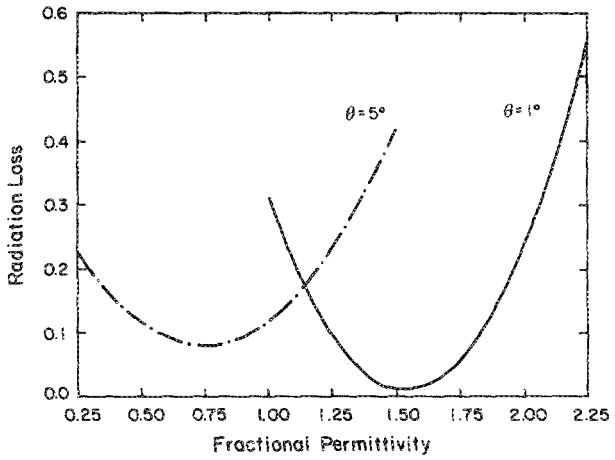

FIG. 4. Calculated radiation loss as a function of fractional permittivity (χ) for intersecting waveguides with small ($\theta = 1°$) and large ($\theta = 5°$) angles.

Fig. 2. From these results it follows that at small intersection angles all the interactions represented in Eq. (7) are significant. However, it also follows from Eqs. (3) and (4) that a reduction in the coupling of guided to radiation modes in the first order implies a similar effect in higher order scattering interactions. As illustrated below, this fact makes the first-order analysis an invaluable design tool.

So far we have restricted our attention to radiation losses in single-Δn intersecting waveguides. The utility of these waveguides at small intersection angles is severely limited due to high losses (see Fig. 2). In a different version of this geometry, namely, the double-Δn [$\chi = 2$, see Eq. (9) below] intersecting waveguides, the losses are somewhat lower.[6] There is no reason to assume that either single-Δn or double-Δn intersecting waveguides represent an optimum geometry with respect to providing low-loss waveguide structures. Therefore, we describe radiation losses in the generalized case of fractional-Δn intersecting waveguides with the permittivity in the intersection region given by

$$\epsilon_{\text{int}} = \epsilon_s + \chi(\epsilon_f - \epsilon_s). \tag{9}$$

The fractional permittivity χ is obtained as a consequence of doping of the intersection region with controlled amounts of titanium. The calculated (first-order analysis) radiation loss as a function of the fractional doping is shown in Fig. 4. Such a dramatic change in radiation loss with fractional permittivity arises due to interference between the evanescent (region I) and guided (region II) contributions to the coupling coefficient between guided and radiation modes.[4] Note that for an optical switch with a small intersection angle $\theta = 1°$, the radiation losses are virtually eliminated for $\chi \approx 1.5$. However, the fractional doping has a smaller effect in reducing the losses in large-angle crossovers, for example, $\theta = 5°$. It is important to realize that other variations of intersecting waveguides may prove more effective as large-angle crossovers.

In summary, multiple scattering analysis provides for the first time an explanation for radiation loss measurements in intersecting waveguides and also provides a predictive capability to design low-loss structures. This research was supported by the National Science Foundation under grants ECE-8508024 and EET-8802713.

[1]A. Neyer, Electron. Lett. **19**, 553 (1983).
[2]G. A. Bogert, Electron. Lett. **23**, 72 (1987).
[3]N. Agrawal, L. McCaughan, and S. R. Seshadri, J. Appl. Phys. **62**, 2187 (1987).
[4]N. Agrawal and L. McCaughan, J. Appl. Phys. (to be published).
[5]L. McCaughan, N. Agrawal, and G. A. Bogert, Appl. Phys. Lett. **51**, 1389 (1987).
[6]E. E. Bergmann, L. McCaughan, and J. E. Watson, Appl. Opt. **23**, 3000 (1984).
[7]A. Neyer, W. Mevenkamp, L. Thylen, and B. Lagerström, J. Lightwave Technol. **LT-3**, 635 (1985).
[8]N. Agrawal (unpublished).